Search for Pair Production of Scalar Top Quarks Decaying to a τ Lepton and a b Quark in $p\bar{p}$ Collisions at $\sqrt{s} = 1.96$ TeV

T. Aaltonen,[23] J. Adelman,[13] T. Akimoto,[54] M.G. Albrow,[17] B. Álvarez González,[11] S. Amerio,[42] D. Amidei,[34] A. Anastassov,[51] A. Annovi,[19] J. Antos,[14] M. Aoki,[24] G. Apollinari,[17] A. Apresyan,[47] T. Arisawa,[56] A. Artikov,[15] W. Ashmanskas,[17] A. Attal,[3] A. Aurisano,[52] F. Azfar,[41] P. Azzi-Bacchetta,[42] P. Azzurri,[45] N. Bacchetta,[42] W. Badgett,[17] A. Barbaro-Galtieri,[28] V.E. Barnes,[47] B.A. Barnett,[25] S. Baroiant,[7] V. Bartsch,[30] G. Bauer,[32] P.-H. Beauchemin,[33] F. Bedeschi,[45] P. Bednar,[14] S. Behari,[25] G. Bellettini,[45] J. Bellinger,[58] A. Belloni,[22] D. Benjamin,[16] A. Beretvas,[17] J. Beringer,[28] T. Berry,[29] A. Bhatti,[49] M. Binkley,[17] D. Bisello,[42] I. Bizjak,[30] R.E. Blair,[2] C. Blocker,[6] B. Blumenfeld,[25] A. Bocci,[16] A. Bodek,[48] V. Boisvert,[48] G. Bolla,[47] A. Bolshov,[32] D. Bortoletto,[47] J. Boudreau,[46] A. Boveia,[10] B. Brau,[10] A. Bridgeman,[24] L. Brigliadori,[5] C. Bromberg,[35] E. Brubaker,[13] J. Budagov,[15] H.S. Budd,[48] S. Budd,[24] K. Burkett,[17] G. Busetto,[42] P. Bussey,[21] A. Buzatu,[33] K. L. Byrum,[2] S. Cabrera^{r},[16] M. Campanelli,[35] M. Campbell,[34] F. Canelli,[17] A. Canepa,[44] D. Carlsmith,[58] R. Carosi,[45] S. Carrillo^{l},[18] S. Carron,[33] B. Casal,[11] M. Casarsa,[17] A. Castro,[5] P. Catastini,[45] D. Cauz,[53] M. Cavalli-Sforza,[3] A. Cerri,[28] L. Cerrito^{p},[30] S.H. Chang,[27] Y.C. Chen,[1] M. Chertok,[7] G. Chiarelli,[45] G. Chlachidze,[17] F. Chlebana,[17] K. Cho,[27] D. Chokheli,[15] J.P. Chou,[22] G. Choudalakis,[32] S.H. Chuang,[51] K. Chung,[12] W.H. Chung,[58] Y.S. Chung,[48] C.I. Ciobanu,[24] M.A. Ciocci,[45] A. Clark,[20] D. Clark,[6] G. Compostella,[42] M.E. Convery,[17] J. Conway,[7] B. Cooper,[30] K. Copic,[34] M. Cordelli,[19] G. Cortiana,[42] F. Crescioli,[45] C. Cuenca Almenar^{r},[7] J. Cuevas^{o},[11] R. Culbertson,[17] J.C. Cully,[34] D. Dagenhart,[17] M. Datta,[17] T. Davies,[21] P. de Barbaro,[48] S. De Cecco,[50] A. Deisher,[28] G. De Lentdecker^{d},[48] G. De Lorenzo,[3] M. Dell'Orso,[45] L. Demortier,[49] J. Deng,[16] M. Deninno,[5] D. De Pedis,[50] P.F. Derwent,[17] G.P. Di Giovanni,[43] C. Dionisi,[50] B. Di Ruzza,[53] J.R. Dittmann,[4] M. D'Onofrio,[3] S. Donati,[45] P. Dong,[8] J. Donini,[42] T. Dorigo,[42] S. Dube,[51] J. Efron,[38] R. Erbacher,[7] D. Errede,[24] S. Errede,[24] R. Eusebi,[17] H.C. Fang,[28] S. Farrington,[29] W.T. Fedorko,[13] R.G. Feild,[59] M. Feindt,[26] J.P. Fernandez,[31] C. Ferrazza,[45] R. Field,[18] G. Flanagan,[47] R. Forrest,[7] S. Forrester,[7] M. Franklin,[22] J.C. Freeman,[28] I. Furic,[18] M. Gallinaro,[49] J. Galyardt,[12] F. Garberson,[10] J.E. Garcia,[45] A.F. Garfinkel,[47] K. Genser,[17] H. Gerberich,[24] D. Gerdes,[34] S. Giagu,[50] V. Giakoumopolou^{a},[45] P. Giannetti,[45] K. Gibson,[46] J.L. Gimmell,[48] C.M. Ginsburg,[17] N. Giokaris^{a},[15] M. Giordani,[53] P. Giromini,[19] M. Giunta,[45] V. Glagolev,[15] D. Glenzinski,[17] M. Gold,[36] N. Goldschmidt,[18] A. Golossanov,[17] G. Gomez,[11] G. Gomez-Ceballos,[32] M. Goncharov,[52] O. González,[31] I. Gorelov,[36] A.T. Goshaw,[16] K. Goulianos,[49] A. Gresele,[42] S. Grinstein,[22] C. Grosso-Pilcher,[13] R.C. Group,[17] U. Grundler,[24] J. Guimaraes da Costa,[22] Z. Gunay-Unalan,[35] C. Haber,[28] K. Hahn,[32] S.R. Hahn,[17] E. Halkiadakis,[51] A. Hamilton,[20] B.-Y. Han,[48] J.Y. Han,[48] R. Handler,[58] F. Happacher,[19] K. Hara,[54] D. Hare,[51] M. Hare,[55] S. Harper,[41] R.F. Harr,[57] R.M. Harris,[17] M. Hartz,[46] K. Hatakeyama,[49] J. Hauser,[8] C. Hays,[41] M. Heck,[26] A. Heijboer,[44] B. Heinemann,[28] J. Heinrich,[44] C. Henderson,[32] M. Herndon,[58] J. Heuser,[26] S. Hewamanage,[4] D. Hidas,[16] C.S. Hill^{c},[10] D. Hirschbuehl,[26] A. Hocker,[17] S. Hou,[1] M. Houlden,[29] S.-C. Hsu,[9] B.T. Huffman,[41] R.E. Hughes,[38] U. Husemann,[59] J. Huston,[35] J. Incandela,[10] G. Introzzi,[45] M. Iori,[50] A. Ivanov,[7] B. Iyutin,[32] E. James,[17] B. Jayatilaka,[16] D. Jeans,[50] E.J. Jeon,[27] S. Jindariani,[18] W. Johnson,[7] M. Jones,[47] K.K. Joo,[27] S.Y. Jun,[12] J.E. Jung,[27] T.R. Junk,[24] T. Kamon,[52] D. Kar,[18] P.E. Karchin,[57] Y. Kato,[40] R. Kephart,[17] U. Kerzel,[26] V. Khotilovich,[52] B. Kilminster,[38] D.H. Kim,[27] H.S. Kim,[27] J.E. Kim,[27] M.J. Kim,[17] S.B. Kim,[27] S.H. Kim,[54] Y.K. Kim,[13] N. Kimura,[54] L. Kirsch,[6] S. Klimenko,[18] M. Klute,[32] B. Knuteson,[32] B.R. Ko,[16] S.A. Koay,[10] K. Kondo,[56] D.J. Kong,[27] J. Konigsberg,[18] A. Korytov,[18] A.V. Kotwal,[16] J. Kraus,[24] M. Kreps,[26] J. Kroll,[44] N. Krumnack,[4] M. Kruse,[16] V. Krutelyov,[10] T. Kubo,[54] S. E. Kuhlmann,[2] T. Kuhr,[26] N.P. Kulkarni,[57] Y. Kusakabe,[56] S. Kwang,[13] A.T. Laasanen,[47] S. Lai,[33] S. Lami,[45] S. Lammel,[17] M. Lancaster,[30] R.L. Lander,[7] K. Lannon,[38] A. Lath,[51] G. Latino,[45] I. Lazzizzera,[42] T. LeCompte,[2] J. Lee,[48] J. Lee,[27] Y.J. Lee,[27] S.W. Lee^{q},[52] R. Lefèvre,[20] N. Leonardo,[32] S. Leone,[45] S. Levy,[13] J.D. Lewis,[17] C. Lin,[59] C.S. Lin,[28] J. Linacre,[41] M. Lindgren,[17] E. Lipeles,[9] T.M. Liss,[24] A. Lister,[7] D.O. Litvintsev,[17] T. Liu,[17] N.S. Lockyer,[44] A. Loginov,[59] M. Loreti,[42] L. Lovas,[14] R.-S. Lu,[1] D. Lucchesi,[42] J. Lueck,[26] C. Luci,[50] P. Lujan,[28] P. Lukens,[17] G. Lungu,[18] L. Lyons,[41] J. Lys,[28] R. Lysak,[14] E. Lytken,[47] P. Mack,[26] D. MacQueen,[33] R. Madrak,[17] K. Maeshima,[17] K. Makhoul,[32] T. Maki,[23] P. Maksimovic,[25] S. Malde,[41] S. Malik,[30] G. Manca,[29] A. Manousakis^{a},[15] F. Margaroli,[47] C. Marino,[26] C.P. Marino,[24] A. Martin,[59] M. Martin,[25] V. Martin^{j},[21] M. Martínez,[3] R. Martínez-Ballarín,[31] T. Maruyama,[54] P. Mastrandrea,[50] T. Masubuchi,[54] M.E. Mattson,[57] P. Mazzanti,[5] K.S. McFarland,[48] P. McIntyre,[52] R. McNulty^{i},[29] A. Mehta,[29] P. Mehtala,[23]

S. Menzemer[k],[11] A. Menzione,[45] P. Merkel,[47] C. Mesropian,[49] A. Messina,[35] T. Miao,[17] N. Miladinovic,[6] J. Miles,[32] R. Miller,[35] C. Mills,[22] M. Milnik,[26] A. Mitra,[1] G. Mitselmakher,[18] H. Miyake,[54] S. Moed,[22] N. Moggi,[5] C.S. Moon,[27] R. Moore,[17] M. Morello,[45] P. Movilla Fernandez,[28] J. Mülmenstädt,[28] A. Mukherjee,[17] Th. Muller,[26] R. Mumford,[25] P. Murat,[17] M. Mussini,[5] J. Nachtman,[17] Y. Nagai,[54] A. Nagano,[54] J. Naganoma,[56] K. Nakamura,[54] I. Nakano,[39] A. Napier,[55] V. Necula,[16] C. Neu,[44] M.S. Neubauer,[24] J. Nielsen[f],[28] L. Nodulman,[2] M. Norman,[9] O. Norniella,[24] E. Nurse,[30] S.H. Oh,[16] Y.D. Oh,[27] I. Oksuzian,[18] T. Okusawa,[40] R. Oldeman,[29] R. Orava,[23] K. Osterberg,[23] S. Pagan Griso,[42] C. Pagliarone,[45] E. Palencia,[17] V. Papadimitriou,[17] A. Papaikonomou,[26] A.A. Paramonov,[13] B. Parks,[38] S. Pashapour,[33] J. Patrick,[17] G. Pauletta,[53] M. Paulini,[12] C. Paus,[32] D.E. Pellett,[7] A. Penzo,[53] T.J. Phillips,[16] G. Piacentino,[45] J. Piedra,[43] L. Pinera,[18] K. Pitts,[24] C. Plager,[8] L. Pondrom,[58] X. Portell,[3] O. Poukhov,[15] N. Pounder,[41] F. Prakoshyn,[15] A. Pronko,[17] J. Proudfoot,[2] F. Ptohos[h],[17] G. Punzi,[45] J. Pursley,[58] J. Rademacker[c],[41] A. Rahaman,[46] V. Ramakrishnan,[58] N. Ranjan,[47] I. Redondo,[31] B. Reisert,[17] V. Rekovic,[36] P. Renton,[41] M. Rescigno,[50] S. Richter,[26] F. Rimondi,[5] L. Ristori,[45] A. Robson,[21] T. Rodrigo,[11] E. Rogers,[24] S. Rolli,[55] R. Roser,[17] M. Rossi,[53] R. Rossin,[10] P. Roy,[33] A. Ruiz,[11] J. Russ,[12] V. Rusu,[17] H. Saarikko,[23] A. Safonov,[52] W.K. Sakumoto,[48] G. Salamanna,[50] O. Saltó,[3] L. Santi,[53] S. Sarkar,[50] L. Sartori,[45] K. Sato,[17] A. Savoy-Navarro,[43] T. Scheidle,[26] P. Schlabach,[17] E.E. Schmidt,[17] M.A. Schmidt,[13] M.P. Schmidt,[59] M. Schmitt,[37] T. Schwarz,[7] L. Scodellaro,[11] A.L. Scott,[10] A. Scribano,[45] F. Scuri,[45] A. Sedov,[47] S. Seidel,[36] Y. Seiya,[40] A. Semenov,[15] L. Sexton-Kennedy,[17] A. Sfyrla,[20] S.Z. Shalhout,[57] M.D. Shapiro,[28] T. Shears,[29] P.F. Shepard,[46] D. Sherman,[22] M. Shimojima[n],[54] M. Shochet,[13] Y. Shon,[58] I. Shreyber,[20] A. Sidoti,[45] P. Sinervo,[33] A. Sisakyan,[15] A.J. Slaughter,[17] J. Slaunwhite,[38] K. Sliwa,[55] J.R. Smith,[7] F.D. Snider,[17] R. Snihur,[33] M. Soderberg,[34] A. Soha,[7] S. Somalwar,[51] V. Sorin,[35] J. Spalding,[17] F. Spinella,[45] T. Spreitzer,[33] P. Squillacioti,[45] M. Stanitzki,[59] R. St. Denis,[21] B. Stelzer,[8] O. Stelzer-Chilton,[41] D. Stentz,[37] J. Strologas,[36] D. Stuart,[10] J.S. Suh,[27] A. Sukhanov,[18] H. Sun,[55] I. Suslov,[15] T. Suzuki,[54] A. Taffard[e],[24] R. Takashima,[39] Y. Takeuchi,[54] R. Tanaka,[39] M. Tecchio,[34] P.K. Teng,[1] K. Terashi,[49] J. Thom[g],[17] A.S. Thompson,[21] G.A. Thompson,[24] E. Thomson,[44] P. Tipton,[59] V. Tiwari,[12] S. Tkaczyk,[17] D. Toback,[52] S. Tokar,[14] K. Tollefson,[35] T. Tomura,[54] D. Tonelli,[17] S. Torre,[19] D. Torretta,[17] S. Tourneur,[43] W. Trischuk,[33] Y. Tu,[44] N. Turini,[45] F. Ukegawa,[54] S. Uozumi,[54] S. Vallecorsa,[20] N. van Remortel,[23] A. Varganov,[34] E. Vataga,[36] F. Vázquez[l],[18] G. Velev,[17] C. Vellidis[a],[45] V. Veszpremi,[47] M. Vidal,[31] R. Vidal,[17] I. Vila,[11] R. Vilar,[11] T. Vine,[30] M. Vogel,[36] I. Volobouev[q],[28] G. Volpi,[45] F. Würthwein,[9] P. Wagner,[44] R.G. Wagner,[2] R.L. Wagner,[17] J. Wagner-Kuhr,[26] W. Wagner,[26] T. Wakisaka,[40] R. Wallny,[8] S.M. Wang,[1] A. Warburton,[33] D. Waters,[30] M. Weinberger,[52] W.C. Wester III,[17] B. Whitehouse,[55] D. Whiteson[e],[44] A.B. Wicklund,[2] E. Wicklund,[17] G. Williams,[33] H.H. Williams,[44] P. Wilson,[17] B.L. Winer,[38] P. Wittich[g],[17] S. Wolbers,[17] C. Wolfe,[13] T. Wright,[34] X. Wu,[20] S.M. Wynne,[29] A. Yagil,[9] K. Yamamoto,[40] J. Yamaoka,[51] T. Yamashita,[39] C. Yang,[59] U.K. Yang[m],[13] Y.C. Yang,[27] W.M. Yao,[28] G.P. Yeh,[17] J. Yoh,[17] K. Yorita,[13] T. Yoshida,[40] G.B. Yu,[48] I. Yu,[27] S.S. Yu,[17] J.C. Yun,[17] L. Zanello,[50] A. Zanetti,[53] I. Zaw,[22] X. Zhang,[24] Y. Zheng[b],[8] and S. Zucchelli[5]

(CDF Collaboration*)

[1] *Institute of Physics, Academia Sinica, Taipei, Taiwan 11529, Republic of China*
[2] *Argonne National Laboratory, Argonne, Illinois 60439*
[3] *Institut de Fisica d'Altes Energies, Universitat Autonoma de Barcelona, E-08193, Bellaterra (Barcelona), Spain*
[4] *Baylor University, Waco, Texas 76798*
[5] *Istituto Nazionale di Fisica Nucleare, University of Bologna, I-40127 Bologna, Italy*
[6] *Brandeis University, Waltham, Massachusetts 02254*
[7] *University of California, Davis, Davis, California 95616*
[8] *University of California, Los Angeles, Los Angeles, California 90024*
[9] *University of California, San Diego, La Jolla, California 92093*
[10] *University of California, Santa Barbara, Santa Barbara, California 93106*
[11] *Instituto de Fisica de Cantabria, CSIC-University of Cantabria, 39005 Santander, Spain*
[12] *Carnegie Mellon University, Pittsburgh, PA 15213*
[13] *Enrico Fermi Institute, University of Chicago, Chicago, Illinois 60637*
[14] *Comenius University, 842 48 Bratislava, Slovakia; Institute of Experimental Physics, 040 01 Kosice, Slovakia*
[15] *Joint Institute for Nuclear Research, RU-141980 Dubna, Russia*
[16] *Duke University, Durham, North Carolina 27708*
[17] *Fermi National Accelerator Laboratory, Batavia, Illinois 60510*
[18] *University of Florida, Gainesville, Florida 32611*
[19] *Laboratori Nazionali di Frascati, Istituto Nazionale di Fisica Nucleare, I-00044 Frascati, Italy*
[20] *University of Geneva, CH-1211 Geneva 4, Switzerland*

[21] Glasgow University, Glasgow G12 8QQ, United Kingdom
[22] Harvard University, Cambridge, Massachusetts 02138
[23] Division of High Energy Physics, Department of Physics,
University of Helsinki and Helsinki Institute of Physics, FIN-00014, Helsinki, Finland
[24] University of Illinois, Urbana, Illinois 61801
[25] The Johns Hopkins University, Baltimore, Maryland 21218
[26] Institut für Experimentelle Kernphysik, Universität Karlsruhe, 76128 Karlsruhe, Germany
[27] Center for High Energy Physics: Kyungpook National University,
Daegu 702-701, Korea; Seoul National University, Seoul 151-742,
Korea; Sungkyunkwan University, Suwon 440-746,
Korea; Korea Institute of Science and Technology Information, Daejeon,
305-806, Korea; Chonnam National University, Gwangju, 500-757, Korea
[28] Ernest Orlando Lawrence Berkeley National Laboratory, Berkeley, California 94720
[29] University of Liverpool, Liverpool L69 7ZE, United Kingdom
[30] University College London, London WC1E 6BT, United Kingdom
[31] Centro de Investigaciones Energeticas Medioambientales y Tecnologicas, E-28040 Madrid, Spain
[32] Massachusetts Institute of Technology, Cambridge, Massachusetts 02139
[33] Institute of Particle Physics: McGill University, Montréal,
Canada H3A 2T8; and University of Toronto, Toronto, Canada M5S 1A7
[34] University of Michigan, Ann Arbor, Michigan 48109
[35] Michigan State University, East Lansing, Michigan 48824
[36] University of New Mexico, Albuquerque, New Mexico 87131
[37] Northwestern University, Evanston, Illinois 60208
[38] The Ohio State University, Columbus, Ohio 43210
[39] Okayama University, Okayama 700-8530, Japan
[40] Osaka City University, Osaka 588, Japan
[41] University of Oxford, Oxford OX1 3RH, United Kingdom
[42] University of Padova, Istituto Nazionale di Fisica Nucleare,
Sezione di Padova-Trento, I-35131 Padova, Italy
[43] LPNHE, Universite Pierre et Marie Curie/IN2P3-CNRS, UMR7585, Paris, F-75252 France
[44] University of Pennsylvania, Philadelphia, Pennsylvania 19104
[45] Istituto Nazionale di Fisica Nucleare Pisa, Universities of Pisa,
Siena and Scuola Normale Superiore, I-56127 Pisa, Italy
[46] University of Pittsburgh, Pittsburgh, Pennsylvania 15260
[47] Purdue University, West Lafayette, Indiana 47907
[48] University of Rochester, Rochester, New York 14627
[49] The Rockefeller University, New York, New York 10021
[50] Istituto Nazionale di Fisica Nucleare, Sezione di Roma 1,
University of Rome "La Sapienza," I-00185 Roma, Italy
[51] Rutgers University, Piscataway, New Jersey 08855
[52] Texas A&M University, College Station, Texas 77843
[53] Istituto Nazionale di Fisica Nucleare, University of Trieste/ Udine, Italy
[54] University of Tsukuba, Tsukuba, Ibaraki 305, Japan
[55] Tufts University, Medford, Massachusetts 02155
[56] Waseda University, Tokyo 169, Japan
[57] Wayne State University, Detroit, Michigan 48201
[58] University of Wisconsin, Madison, Wisconsin 53706
[59] Yale University, New Haven, Connecticut 06520

(Dated: February 26, 2008)

We present the results of a search for pair production of scalar top quarks ($\tilde{t}_1$) in an R-parity violating supersymmetric scenario using 322 pb^{-1} of $p\overline{p}$ collisions at $\sqrt{s} = 1.96$ TeV collected by the upgraded Collider Detector at Fermilab. We assume each $\tilde{t}_1$ decays into a τ lepton and a b quark with a branching ratio β, and that the final state contains either an electron or a muon from a leptonic τ decay, a hadronically decaying τ lepton, and two or more jets. Two candidate events pass our final selection criteria, consistent with the expectation from standard model processes. We present upper limits on the cross section times branching ratio squared $\sigma(\tilde{t}_1\bar{\tilde{t}}_1) \times \beta^2$ as a function of the stop mass $m(\tilde{t}_1)$. Assuming $\beta = 1$, we set a 95% confidence level limit $m(\tilde{t}_1) > 153$ GeV/c^2 obtained using a next-to-leading order cross section. These limits are also fully applicable to the case of a pair produced third generation scalar leptoquark decaying into a τ lepton and a b quark.

PACS numbers: 12.60.Jv, 14.80.Ly,13.85.Rm,11.30.Pb,11.30.Er

*With visitors from [a]University of Athens, 15784 Athens, Greece, [b]Chinese Academy of Sciences, Beijing 100864, China, [c]University

In supersymmetric (SUSY) models [1], the spin-1/2 quarks and leptons have spin-0 quark and lepton partners. Experimental data suggest that the superpartners of the first and second generation are massive with masses greater than those of the standard model particles, while the mass of the lighter scalar top quark (stop or $\tilde{t}_1$) is weakly constrained and can be below that of the top quark [2]. This is due to the mixing between the left and right handed interaction eigenstates which is a function of the large Yukawa coupling of the top quark. At the Fermilab Tevatron stop quarks and antiquarks can be produced in pairs in strong interactions ($gg/q\bar{q}\to\tilde{t}_1\bar{\tilde{t}}_1$). A single stop could also be produced at the Tevatron, e.g., via $bg\to\tilde{t}_1\tau$ [3]; however, unlike pair production, this process requires an R-parity (R_p) violating vertex. In regions of parameter space not excluded by data, R_p violating ($\not{R}_p$) couplings are small [4], making single stop production negligible compared to pair production. Stop quarks can decay into lighter SUSY and standard model (SM) particles if R_p is conserved or into ordinary quarks and/or leptons if R_p is violated. Within the framework of $\not{R}_p$ SUSY [4], theoretical studies indicate that the dominant decay mode for the light stop is the lepton number violating decay $\tilde{t}_1\to\tau b$ for a wide range of SUSY model parameters, including the region allowed by neutrino oscillation data [5]. We set an upper limit on the cross section $\sigma(\tilde{t}_1\bar{\tilde{t}}_1)\times\beta^2$, neglecting additional decay modes that may pass selections of this analysis when $\beta\equiv\mathcal{B}(\tilde{t}_1\to\tau b)<1$. To set 95% confidence level limits (C.L.) on the stop mass $m(\tilde{t}_1)$, we assume that $\beta=1$. Note that our procedure is conservative even if the contributions from other decay modes are not negligible as it will yield less stringent limits.

Since third generation scalar leptoquarks (LQ_3) are also expected to decay into τ and b, the search for $\not{R}_p$ stop pair production is also sensitive to leptoquark production. Leptoquarks appear in various SM extensions [6], and $\mathcal{B}(LQ_3\to\tau b)=1$ for all LQ_3 states when $m(LQ_3)<m(t)$. Contrary to $LQ_3\overline{LQ}_3$ production, stop pair production also involves diagrams with virtual gluino exchange which are, however, strongly suppressed if gluino mass is high. For the existing limits on gluino mass [7] the next-to-leading order (NLO) cross section for $LQ_3\overline{LQ}_3$ is very close to that for $\tilde{t}_1\bar{\tilde{t}}_1$. Thus, the limit results obtained for $\not{R}_p$ stop should be fully applicable to the case of LQ_3 pair production.

In this Letter we describe a search for $\tilde{t}_1\bar{\tilde{t}}_1\to\tau^+\tau^- b\bar{b}$ with the CDF II detector [8]. We look for a final state with either an electron or muon from the decay $\tau\to\ell\nu_\ell\nu_\tau$ ($\ell=\ e$ or μ), a hadronically decaying tau $\tau_{\rm h}$, missing transverse energy $\not\!\!E_T$ [9] from the neutrinos, and two or more jets. We have studied the addition of a requirement that the jets are consistent with originating from the hadronization of a b quark but found that the increase in purity is outweighed by the loss in signal acceptance. Therefore, we make no such specific requirement. This analysis uses approximately three times more data and a higher $\sqrt{s}$ than the previous CDF result [10] that set a 95% C.L. limit of $m(\tilde{t}_1)>122$ GeV/c^2. The increased $\sqrt{s}$ is expected to give a substantial increase in $\tilde{t}_1\bar{\tilde{t}}_1$ production rate, e.g. for $m(\tilde{t}_1)=155$ GeV/c^2 the cross-section grows by $\sim 35\%$.

Improvements to the CDF II detector include the upgraded trigger system that allows more efficient data selection with dedicated trigger paths for events with two taus [11] and the upgraded muon detectors that provide better coverage and increased acceptance.

CDF II is a large general-purpose detector for studying particles produced in $p\overline{p}$ collisions [8], and features several main subsystems critical to this analysis. The charged particle tracking system, consisting of multilayer silicon detectors and a large open-cell cylindrical drift chamber (COT). At $|\eta|<1$ [9] charged particle trajectories traverse all chamber layers, while at larger $|\eta|$ the chamber coverage is reduced progressively. The COT is enclosed in a 1.4 T superconducting magnet. The calorimeter system is organized into electromagnetic and hadronic sections segmented in a projective tower geometry and covers $|\eta|<3.6$. A set of strip and wire chambers (CES) is located within the central electromagnetic (CEM) calorimeter at approximately the depth of shower maximum and aids in reconstructing electrons, photons, and $\pi^0\to\gamma\gamma$ decays for $|\eta|<1.1$. The central muon detection system is located outside of the calorimeter and covers $|\eta|<1.0$ with two subsystems: the central muon (CMUP, $|\eta|<0.6$) and central muon system extension (CMX, $0.6<|\eta|<1.0$).

The analysis begins with a data sample collected by inclusive lepton-plus-track triggers [11]. CDF II uses a three-level trigger system. At levels 1 and 2 the lepton-plus-track triggers require an electron candidate with calorimeter cluster $E_T>8$ GeV (in CEM) or a muon candidate (in CMUP or in CMX) with track momentum $p_T>8$ GeV/c and a second track with $p_T>5$ GeV/c.

of Bristol, Bristol BS8 1TL, United Kingdom, [d]University Libre de Bruxelles, B-1050 Brussels, Belgium, [e]University of California Irvine, Irvine, CA 92697, [f]University of California Santa Cruz, Santa Cruz, CA 95064, [g]Cornell University, Ithaca, NY 14853, [h]University of Cyprus, Nicosia CY-1678, Cyprus, [i]University College Dublin, Dublin 4, Ireland, [j]University of Edinburgh, Edinburgh EH9 3JZ, United Kingdom, [k]University of Heidelberg, D-69120 Heidelberg, Germany, [l]Universidad Iberoamericana, Mexico D.F., Mexico, [m]University of Manchester, Manchester M13 9PL, England, [n]Nagasaki Institute of Applied Science, Nagasaki, Japan, [o]University de Oviedo, E-33007 Oviedo, Spain, [p]Queen Mary, University of London, London, E1 4NS, England, [q]Texas Tech University, Lubbock, TX 79409, [r]IFIC(CSIC-Universitat de Valencia), 46071 Valencia, Spain,

Tracks at these trigger levels are identified by the fast online tracker (XFT) [12] in $|\eta| < 1$. At level 3, where the full software event reconstruction is performed, the second track is required to be consistent with originating from a tau decay by demanding that there be no other nearby tracks with $p_T > 1.5$ GeV/c between the cones of 0.175 and 0.524 radians around the track. The integrated luminosity of the data sample is 322 ± 19 pb^{-1} (304 ± 18 pb^{-1}) for CEM and CMUP (CMX) [13].

From the trigger sample we select events offline by identifying at least one lepton with ${p_T}^{\ell} > 10$ GeV/c and at least one $\tau_{\rm h}$ candidate in $|\eta| < 1$. The details of the $\tau_{\rm h}$ and π^0 identification algorithms can be found in Ref. [14]. The tracks contributing to a $\tau_{\rm h}$ candidate must satisfy the following requirements: the highest p_T track ("seed track") is required to have $p_T > 6$ GeV/c; the other tracks must have $p_T > 1$ GeV/c and be within a tau track signal cone [15]. The contributing π^0 candidates are required to have $E_T > 1$ GeV and to be within a π^0 signal cone of 0.17 radians with respect to the seed track. The track and π^0 isolation regions are defined as annuli between the respective signal cones and the cone of 0.52 rad around the seed track. We require that there be zero tracks with $p_T > 1$ GeV/c in the track isolation region and that the sum of the transverse energies of the π^0 candidates in the π^0 isolation region be less than 0.6 GeV. The $\tau_{\rm h}$ candidate visible 4−momentum is defined as $p^{\tau} \equiv \sum p^{track} + \sum p^{\pi^0}$, where $\sum p^{track}$ and $\sum p^{\pi^0}$ are the sums of momenta of tracks and π^0 candidates in their respective signal cones. We require the transverse component of the visible momentum p_T^{τ} to be greater than 15 GeV/c. Jets in this analysis are reconstructed using a fixed-cone algorithm with $\Delta R \equiv \sqrt{\Delta\eta^2 + \Delta\phi^2} = 0.4$ within $|\eta| < 2.4$.

We apply a series of event selection cuts designed to improve the sensitivity of the search by reducing the dominant SM backgrounds. These backgrounds include QCD multijet events, vector boson production with multiple jets, and $t\bar{t}$ production. In QCD multijet events, for example, semileptonic b quark decays or γ conversions can be misidentified as lepton signal candidates, and narrow jets can be misidentified as tau candidates. We require leptons to be isolated to reduce the QCD background: the sum of the p_T of the tracks within $\Delta R < 0.4$ around the $\tilde{t}_1$ decay lepton candidate, which we denote as I_{trk}, must be less than 2 GeV/c, and there must be no jet with $E_T > 15$ GeV whose axis is in an annulus of $0.3 < \Delta R < 0.8$ around the lepton. Further, we reject events where the muon or electron candidate is consistent with a cosmic ray muon or photon conversion electron (see Ref. [14] for details). To suppress the contribution of $Z^0 \to \ell^+\ell^-$, we veto events where the invariant mass of the primary electron (muon) and a reconstructed electron (muon) candidate, which is required to pass only very loose identification criteria [14], is $76 < m_{\ell\ell} < 106$ GeV/c^2. We also reject events where the invariant mass of the electron candidate and its hadronic tau partner is $76 < m_{e\tau} < 106$ GeV/c^2 and they are azimuthally separated with $|\Delta\phi_{e\tau}| > 2.9$ rad. For the muon channel we do not apply a similar requirement, as the probability for a muon to be reconstructed as a $\tau_{\rm h}$ is negligible. To suppress further QCD multijet and $Z^0 \to \tau^+\tau^-$ events [10], we require $S_T \equiv (|{p_T}^{\ell}| + |{p_T}^{\tau_{\rm h}}| + |\not\!\!E_T|/c) > 110$ GeV/c.

We define six regions in the $m_T(\ell, \not\!\!E_T) \equiv \sqrt{2{p_T}^{\ell}\not\!\!E_T(1 - \cos\Delta\phi_{\ell,\not\!\!E_T})}$ versus $N_{\rm jet}$ plane, and denote them as A_j (B_j) for $m_T \leq 35$ GeV/c^2 ($m_T > 35$ GeV/c^2) and $j = 0$, 1 or 2 for $N_{\rm jet} = 0$, 1 or ≥ 2. We count into $N_{\rm jet}$ the jet candidates that have $E_T > 20$ GeV and are separated from any of e, μ or $\tau_{\rm h}$ by $\Delta R > 0.8$. The values of minimal S_T and jet E_T thresholds are optimized for maximum significance in the A_2 region for a stop mass in the range of $140 - 160$ GeV/c^2. The $m_T \leq 35$ GeV/c^2 division effectively separates signal from W + jet and $t\bar{t}$ backgrounds. The requirement of $N_{\rm jet} \geq 2$ strongly suppresses the contribution of Drell-Yan backgrounds but keeps most signal events which are expected to have two or more jets. Studies using PYTHIA [16] with the GEANT3-based [17] CDF II detector simulation show that 58% of the signal events satisfying all other selection requirements fall into the region A_2 (for a stop mass of 150 GeV/c^2), while for the SM background expectation the corresponding fraction is 5.6%. The data in the region A_2 were not examined until the analysis procedure was finalized. The regions with $N_{\rm jet} = 0$ or 1 contain mostly background and were used mainly as control samples for validation. Region B_2 has an appreciable signal acceptance ($\sim 40\%$ of that in region A_2) but substantially higher background expectation. For statistical interpretation of the data, we developed a likelihood method that, in addition to our primary signal region A_2, utilizes side-band regions A_0, B_0, and B_2, which are used to perform data-driven W + jet background estimations and to improve the sensitivity of the analysis.

The total event acceptance is $\alpha \equiv A_{\rm geom} \cdot A_{\rm kin} \cdot \epsilon_{\rm ID} \cdot \epsilon_{\rm ISO} \cdot \epsilon_{\rm trig} \cdot \epsilon_{\rm other}$. Here $A_{\rm geom} \cdot A_{\rm kin}$ is the product of geometrical and kinematical acceptances, $\epsilon_{\rm ID}$ is the combined efficiency to identify lepton and $\tau_{\rm h}$ candidates, $\epsilon_{\rm ISO}$ is the combined efficiency for lepton and $\tau_{\rm h}$ isolation requirements, $\epsilon_{\rm trig}$ is the combined lepton and XFT track trigger efficiency, and $\epsilon_{\rm other}$ is the efficiency for the all remaining cuts. We use Monte Carlo simulation to calculate $A_{\rm geom} \cdot A_{\rm kin}$, $\epsilon_{\rm ID}$, $\epsilon_{\rm ISO}$, and $\epsilon_{\rm other}$. In the simulation we use CTEQ5L [18] for the parton distribution functions (PDFs) and the renormalization scale Q is given by $Q = \sqrt{m(\tilde{t}_1)^2 + p_T(\tilde{t}_1)^2}$. The trigger efficiencies are measured using data. In region A_2 α increases nearly linearly from about 0.6% at $m(\tilde{t}_1) = 100$ GeV/c^2 to 2.7% at $m(\tilde{t}_1) = 170$ GeV/c^2 and is similar for both electron and muon channels.

The combined systematic uncertainty on the total event acceptance for the electron (muon) channel decreases almost linearly from 11.1% (10.9%) for a stop mass of $m(\tilde{t}_1)$= 100 GeV/c^2 to 6.9% (7.5%) for 170 GeV/c^2. The largest contribution comes from the PDF systematic uncertainty, which is estimated using the uncertainty sets of CTEQ6.1M PDFs [19] and the technique described in [20]. For a 150 GeV/c^2 stop in the electron (muon) channel this uncertainty is 3.8% (4.1%) of the total event acceptance. The uncertainty due to imperfect knowledge of the jet energy scale, determined by varying the jet energy corrections by $\pm 1\sigma$, is 3.5% (2.3%). The uncertainty due to the amount of initial and final state radiation is found to be 2.5%. Other sources of systematic error include the uncertainties in lepton and $\tau_{\rm h}$ identification and isolation, Monte Carlo simulation, and $\not\!\!E_T$ resolution, and amount to a 4.7% (5.5%) relative contribution in the electron (muon) channel. The uncertainty on the integrated luminosity of the data sample is 6%.

The SM backgrounds come from two sources: (i) events with a true $\ell\tau_{\rm h}$ pair from $Z^0/\gamma^*(\rightarrow\tau^+\tau^-)$+jets, $t\bar{t}$ and diboson (W^+W^-, $W^\pm Z^0$, Z^0Z^0) production; and (ii) events where lepton or $\tau_{\rm h}$ candidates do not originate from a true lepton or tau but from the jets in W + jet, $Z^0/\gamma^*(\rightarrow\ell^+\ell^-)$+jets and QCD multijet events. We first estimate the background from SM processes excluding the W + jet contribution. $Z^0/\gamma^*(\rightarrow\tau^+\tau^-)$+jets, $Z^0/\gamma^*(\rightarrow\ell^+\ell^-)$+jets, $t\bar{t}$, and W^+W^- production are estimated using PYTHIA and the CDF II detector simulation. For Drell-Yan backgrounds we use scale factors that improve the agreement between the prediction for the yield of these events in Monte Carlo simulation and the yield observed in data. The QCD multijet contribution is estimated by extrapolating the number of observed events in data for events with non-isolated leptons, defined by 2 GeV/c < I_{trk} < 10 GeV/c, into the class of events with an isolated lepton, defined by I_{trk} < 2 GeV/c [14]. The NLO cross sections of 6.7 ± 0.7 pb [21] and 13.5 ± 0.5 pb [22] for $t\bar{t}$ and W^+W^- production, respectively, are used. The contributions from $W^\pm Z^0$ and Z^0Z^0 are found to be negligible.

The PYTHIA Monte Carlo simulation is not expected to accurately predict the absolute rate of the W + jet background contribution in this analysis. Apart from other considerations, such an estimate relies on the probability for a jet to be identified as a tau candidate which is known not to be well predicted by PYTHIA [14]. Therefore, to estimate the W + jet contribution N^{W+j} in each region, we use the differences between the data and all other backgrounds plus signal in regions A_2, B_2, A_0, and B_0 and the assumption that $\mathcal{R} \equiv \left[N^{W+j}(A_2)/N^{W+j}(B_2)\right] \cdot \left[N^{W+j}(B_0)/N^{W+j}(A_0)\right] \sim 1$. While the absolute W + jet rates from PYTHIA Monte Carlo simulation are unreliable, the ratios in $\mathcal{R}$ are determined by kinematics of the W + jet events at fixed $N_{\rm jet}$ and are well modeled in MC. Based on MC predictions and cross checks with data vs MC comparisons, we conclude that $\mathcal{R} = 1.0 \pm 0.5$ is a conservative assumption. We define a likelihood function using Poisson statistics as a function of the $\tilde{t}_1\bar{\tilde{t}}_1$ production cross section (σ) and N^{W+j}. The input parameters to the likelihood are the numbers of observed and expected events in each of the four regions. The number of expected events in region i is given by $N_i = \sigma \cdot \mathcal{B}(\tau\tau\rightarrow\ell\tau_{\rm h}) \cdot \int \mathcal{L}\, dt \cdot \alpha_i + N_i^{\rm BG} + N_i^{W+j}$, where the branching ratio $\mathcal{B}(\tau\tau\rightarrow\ell\tau_{\rm h}) \simeq 0.23$, $N_i^{\rm BG}$ includes all SM backgrounds except W + jet events, and α_i is the total event acceptance for signal in region i. Note that α_i is negligibly small for regions A_0 and B_0. The ratio $\mathcal{R} = 1.0 \pm 0.5$ and N^{W+j} in regions A_0, B_0, and B_2 are nuisance parameters with flat prior distributions. The large uncertainty on $\mathcal{R}$ does not affect the result because the W + jet contribution in region A_2 is expected to be small. We use this two-dimensional likelihood to estimate the number of W + jet events for each region and to calculate upper limits on $\sigma \times \beta^2$.

TABLE I: Number of events observed in data, $N_{\rm obs}$, along with the expected number of SM background events. Note that the W + jet contributions are obtained from the maxima of likelihoods that depend on the observed number of events in the data, the number of SM events excluding the W + jet contribution, and on the $\tilde{t}_1\bar{\tilde{t}}_1$ production cross section.

	$e + \tau_{\rm h}$ Channel			$\mu + \tau_{\rm h}$ Channel		
Reg	$N_{\rm obs}$	SM Backgrounds		$N_{\rm obs}$	SM Backgrounds	
		Other	W+jet		Other	W+jet
A_2	**1**	$2.0^{+0.5}_{-0.4}$	$0^{+0.4}_{-0}$	**1**	$1.0^{+0.4}_{-0.2}$	$0^{+0.5}_{-0}$
B_2	4	$2.8^{+0.5}_{-0.3}$	$1.0^{+2.0}_{-1.0}$	4	$2.3^{+0.4}_{-0.3}$	$1.7^{+2.0}_{-1.5}$
A_1	4	$3.3^{+0.5}_{-0.5}$	$0.2^{+1.2}_{-0.2}$	3	$2.6^{+0.6}_{-0.4}$	$0.1^{+0.8}_{-0.1}$
B_1	9	$2.3^{+0.4}_{-0.3}$	$6.7^{+3.2}_{-2.7}$	6	$2.3^{+0.5}_{-0.3}$	$3.8^{+2.7}_{-2.1}$
A_0	11	$9.1^{+1.2}_{-1.1}$	$1.6^{+2.7}_{-1.6}$	8	$5.2^{+0.7}_{-0.5}$	$2.5^{+2.4}_{-2.1}$
B_0	25	$4.5^{+0.7}_{-0.6}$	$21.1^{+5.6}_{-4.3}$	28	$5.4^{+0.8}_{-0.6}$	$23.6^{+4.9}_{-5.7}$

In Table I we show the number of events observed in the data along with the expected number of SM events. The W + jet contributions are shown separately as they are estimated using the observed number of events in the data, the number of SM events excluding the W + jet contribution, and a possible stop quark contribution. In Fig. 1 we present the $N_{\rm jet}$ distribution for events with $m_T \leq 35$ GeV/c^2 (regions A_0, A_1, and A_2).

A total of two events is found in region A_2 which can be compared to the prediction from SM processes of roughly three events (see Table I). With no excess in this region, we calculate a 95% C.L. limit on the $\tilde{t}_1\bar{\tilde{t}}_1$ production cross section. In the likelihood function that was discussed above, we integrate out the W + jet probability distribution to obtain a probability of observing the number of events found in data given a specific signal cross section. The electron and muon channels are treated as two sep-

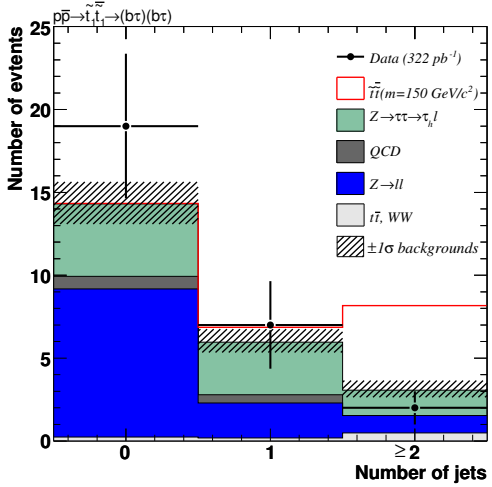

FIG. 1: Event distribution as a function of the number of jets with $E_T > 20$ GeV separated from the lepton and tau candidates for data events with $m_T(\ell, \not\!\!E_T) \leq 35$ GeV/c^2 (regions A_0, A_1, and A_2) compared to the expectations from SM background processes and prediction for $\tilde{t}_1\bar{\tilde{t}}_1$ ($m(\tilde{t}_1) = 150$ GeV/c^2) signal. The SM background processes shown do not include the W + jet contribution.

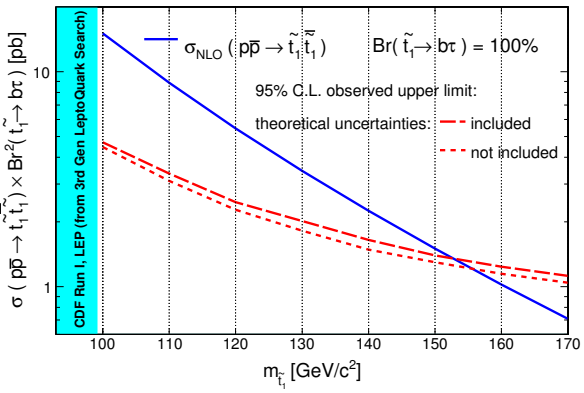

FIG. 2: 95% C.L. limit curves for the $\tilde{t}_1\bar{\tilde{t}}_1$ production cross section times the branching ratio $\tilde{t}_1 \to b\tau$ squared for the cases when the theoretical uncertainty on cross section is (dashed line) and is not (dotted line) considered during calculation of the limit (see text for details). A previous constraint obtained from CDF and LEP leptoquark searches ($m(LQ_3) > 99$ GeV/c^2) [23] is also shown.

TABLE II: 95% C.L. upper limit on $\sigma(\tilde{t}_1\bar{\tilde{t}}_1) \times \beta^2$ (in pb) as a function of $m(\tilde{t}_1)$ for the cases when theoretical uncertainty on the cross section is considered ($\sigma^{95\%}_{with\ uncert} \times \beta^2$) and is not considered ($\sigma^{95\%}_{no\ uncert} \times \beta^2$), where $\beta \equiv \mathcal{B}(\tilde{t}_1 \to \tau b)$.

$m(\tilde{t}_1)$ (GeV/c^2)	100	110	120	130	140	150	160	170
$\sigma^{95\%}_{with\ uncert} \times \beta^2$ (pb)	4.73	3.37	2.50	1.99	1.61	1.38	1.26	1.14
$\sigma^{95\%}_{no\ uncert} \times \beta^2$ (pb)	4.48	3.11	2.27	1.81	1.47	1.26	1.16	1.04

arate measurements taking into account the correlations among the systematic uncertainties.

Figure 2 and Table II show the 95% C.L. limit on $\sigma(\tilde{t}_1\bar{\tilde{t}}_1) \times \beta^2$ as a function of $m(\tilde{t}_1)$. Figure 2 compares this limit (dotted line) to the NLO cross sections obtained using PROSPINO version 2 [24], our nominal choice of CTEQ6.1M PDFs [19], and a renormalization scale of $Q = \sqrt{m(\tilde{t}_1)^2 + p_T(\tilde{t}_1)^2}$ (solid line). The theoretical uncertainty of ±18% on the cross section is due to the choice of Q (varying the scale from its nominal value by a factor of two or a half) and PDFs. Taking this uncertainty into consideration, the limit calculation provides a 95% C.L. upper limit on $\sigma(\tilde{t}_1\bar{\tilde{t}}_1) \times \beta^2$ which is shown in Fig. 2 using a dashed line. The corresponding mass limit is $m(\tilde{t}_1) > 153$ GeV/c^2. The limit is 156 GeV/c^2 if we do not include the theory uncertainties, and this value can be compared to earlier results.

In conclusion, we have searched for $\tilde{t}_1\bar{\tilde{t}}_1$ production in the final state of a lepton (e or μ), a hadronically decaying tau, and two jets using 322 pb^{-1} of $p\overline{p}$ collision data at $\sqrt{s}$ = 1.96 TeV. The same final state would also be expected within a LQ_3 scenario in addition to an $\not\!\!R_p$ SUSY scenario. We observed no excess of events in data over the number of expected events from SM processes. Therefore, taking into account the theoretical uncertainties on the NLO cross section and assuming $\mathcal{B}(\tilde{t}_1 \to \tau b) = 1$, we set a 95% C.L. lower limit on the $\tilde{t}_1$ mass of 153 GeV/c^2. These results are also applicable to LQ_3 pair production.

We thank the Fermilab staff and the technical staffs of the participating institutions for their vital contributions. This work was supported by the U.S. Department of Energy and National Science Foundation; the Italian Istituto Nazionale di Fisica Nucleare; the Ministry of Education, Culture, Sports, Science and Technology of Japan; the Natural Sciences and Engineering Research Council of Canada; the National Science Council of the Republic of China; the Swiss National Science Foundation; the A.P. Sloan Foundation; the Bundesministerium für Bildung und Forschung, Germany; the Korean Science and Engineering Foundation and the Korean Research Foundation; the Science and Technology Facilities Council and the Royal Society, UK; the Institut National de Physique Nucleaire et Physique des Particules/CNRS; the Russian Foundation for Basic Research; the Comisión Interministerial de Ciencia y Tecnología, Spain; the European Community's Human Potential Programme; the Slovak R&D Agency; and the Academy of Finland.

[1] H.P. Nilles, Phys. Rep. **110**, 1 (1984); H.E. Haber and G.L. Kane, *ibid.* **117**, 75 (1985).

[2] K. Inoue, A. Kakuo, H. Komatsu, and H. Takeshita, Prog. Theor. Phys **68**, 927 (1982); *ibid.* **71**, 413 (1984); L. Ibanez and C. Lopez, Nucl. Phys. B **233**, 511 (1984); J. Ellis and S. Rudaz, Phys. Lett. B **128**, 248 (1983).

[3] A. Alves, O. Eboli and T. Plehn, Phys. Lett. B **558**, 165 (2003).

[4] S. Weinberg, Phys. Rev. D **26**, 287 (1982); G. Farrar and S. Weinberg, *ibid.* **27**, 2732 (1983); S. Dawson, Nucl. Phys. B **261**, 297 (1985). For a recent review on R_p violating SUSY, see R. Barbier *et al.*, Phys. Rep. **420**, 1 (2005).

[5] F. de Campos *et al.*, "R-parity violating decays of the top-quark and the top-squark at the Tevatron," hep-ph/9903245; D. Restrepo, W. Porod, and J. W. F. Valle, Phys. Rev. D **64**, 055011 (2001); S. P. Das, A. Datta, and S. Poddar, Phys. Rev. D **73**, 075014 (2006).

[6] For a review on models with leptoquarks, see S. Davidson, D. C. Bailey and B. A. Campbell, Z. Phys. C **61**, 613 (1994).

[7] V. M. Abazov *et al.* (D0 Collaboration), Phys. Lett. B **638**, 119 (2006). For example, the difference in $\sigma(\tilde{t}_1\bar{\tilde{t}}_1)$ for the case of gluino mass of 200 GeV/c^2 and the case of a very heavy gluino is 3% (for $m(\tilde{t}_1) = 150$ GeV/c^2).

[8] D. Acosta *et al.* (CDF Collaboration), Phys. Rev. D **71**, 032001 (2005).

[9] We use a coordinate system where θ and ϕ are the polar and azimuthal angles, respectively, with respect to the proton beam direction (z axis). The pseudorapidity η is defined as $-\ln[\tan(\theta/2)]$. The transverse momentum of a particle is denoted as $p_T = p\sin\theta$. The analogous quantity using energies, defined as $E_T = E\sin\theta$, is called transverse energy. The uncorrected missing transverse energy, $\not\!\!E_T{}^{unc}$, is the magnitude of $\vec{\not\!\!E}_T{}^{unc} \equiv -\sum E_T^i\,\hat{n}_i$, where $\hat{n}_i$ is the unit vector in the transverse plane pointing from the interaction point to the energy deposition in calorimeter cell i. $\not\!\!E_T$ is $\not\!\!E_T{}^{unc}$ further corrected for the muon p_T and for the effects of non-ideal response of the calorimeter to e, τ, and jets.

[10] D. Acosta *et al.* (CDF Collaboration), Phys. Rev. Lett. **92**, 051803 (2004).

[11] A. Anastassov *et al.*, Nucl. Instrum. MethodsA **518**, 609 (2004).

[12] E.J. Thomson *et al.*, IEEE Trans. Nucl. Sci. **49**, 1063 (2002).

[13] D. Acosta *et al.*, Nucl. Instrum. Methods A **494** (2002) 57; S. Klimenko *et al.*, FERMILAB-FN-0741 (2003).

[14] A. Abulencia *et al.* (CDF Collaboration), Phys. Rev. D **75**, 092004 (2007).

[15] Tau track signal cone is defined as a cone with an opening angle $min[0.17, max(5\text{ GeV}/E_{clu}, 0.05)]$ around the seed track.

[16] T. Sjöstrand *et al.*, Comput. Phys. Commun. **135**, 238 (2001). We use PYTHIA version 6.216.

[17] R. Brun *et al.*, "GEANT3 User's Guide," CERN-DD-EE-81-1 (1989).

[18] H.L. Lai *et al.* (CTEQ Collaboration), Eur. Phys. J. C **12**, 375 (2000).

[19] J. Pumplin *et al.* (CTEQ Collaboration), J. High Energy Phys. **0207**, 012 (2002).

[20] A. Abulencia *et al.* (CDF Collaboration), J. Phys. G **34**, 2457 (2007).

[21] M. Cacciari *et al.*, J. High Energy Phys. **0404**, 68 (2004); N. Kidonakis and R. Vogt, Phys. Rev. D **68**, 114014 (2003).

[22] J. M. Campbell and R. K. Ellis, Phys. Rev. D **60**, 113006 (1999).

[23] F.Abe *et al.* (CDF Collaboration), Phys. Rev. Lett. **79**, 4327 (1997); G. Abbiendi *et al.* (OPAL Collaboration), Eur. Phys. J. C **31**, 281 (2003).

[24] W. Beenakker, R. Höpker, M. Spira, and P. M. Zerwas, Nucl. Phys. B **492**, 51 (1997).